

RESEARCH ARTICLE

Improvement of Fatigue Properties of EN AW 6082 Aluminum Alloy using Different Deep Rolling Directions

M. O. Görtan^{1,2}, and B. Yüksel^{1,2,*}¹Department of Mechanical Engineering, Hacettepe University, 06800 Ankara, Republic of Türkiye²National Nanotechnology Research Center, Bilkent University, 06800 Ankara, Republic of Türkiye

ABSTRACT - Deep rolling (DR) is an effective mechanical surface treatment method to improve the fatigue properties of engineering components. In this method, the surface of the component was rolled using a roller with a predetermined force to obtain reduced roughness, hardness increases and compressive residual stresses in the surface region. These alterations allow for increasing the fatigue lives of the components in industrial applications. In the current study, DR was applied in tangential and longitudinal directions on specimens that were manufactured using EN-AW 6082-T6 aluminum. The resulting roughness, hardness and residual stresses were determined experimentally. Fatigue tests were carried out to determine the improvements in fatigue properties after DR. It was found that DR-induced compressive residual stresses depend on DR direction considerably. Due to this reason, fatigue strength improvements were found to be different for different DR direction applications. Longitudinal rolling resulted in a 23% fatigue strength increase compared to a 7% increase for tangential rolling. For both DR direction applications, fatigue cracks were shown to initiate at the sub-surface region, whereas the as-turned specimens exhibited surface crack initiation.

ARTICLE HISTORY

Received : 15th Aug 2022
Revised : 14th March 2023
Accepted : 12th April 2023
Published : 30th June 2023

KEYWORDS

Fatigue,
6082 Aluminum,
Residual stress,
Deep rolling

1.0 INTRODUCTION

Emission demands and regulations for the automotive industry have been tightening in recent decades [1]. Therefore, the usage of aluminum alloys in this industry has been increasing. Thanks to their low weight and comparatively high strength, they were able to replace steel for various dynamically loaded components in land vehicles, such as wheel suspension arms [2]. Kukielka et al. [3] stated that fatigue is the most prominent cause of mechanical failures in modern machinery. Since the heat-treatable 6xxx series aluminum alloys are typically used to manufacture dynamically loaded components [2], improving the fatigue strength of these alloys is of significant importance for automotive manufacturers.

Fatigue cracks usually form at the surface of components due to surface irregularities and defects. Purnowidodo et al. [4] showed that higher roughness values for pure aluminum fibre-metal laminates might decrease fatigue life. Therefore, reducing surface roughness is known to be an effective method to improve fatigue life, as stated in Kirkhope et al. [5]. Surface work-hardening is also another effective method to enhance high-cycle fatigue (HCF) life. Since plastic deformation is necessary for the crack initiation phase, the work-hardened layer shifts plastic deformation start to higher stress levels and hinders crack initiation [6]. Apart from the two mentioned strategies, compressive residual stresses were shown to delay crack initiation and micro-crack propagation, which results in significant improvement in high-cycle fatigue life, as shown in the work of Ludian and Wagner [7].

Deep rolling (DR) is an effective mechanical surface treatment method that improves high-cycle fatigue life as it allows work-hardening and induces compressive residual stresses in the surface region. At the same time, additional improvement in surface roughness is observed when suitable process parameters are used [8]. In this method, a roller or ball is used to deform the component surface with a predetermined force. DR is usually applied in high-end components such as jet engine turbine blades [9] because of relatively high process times compared to alternative methods such as shot peening. However, shot peening generally reduces fatigue strength while increasing surface roughness [10].

DR has been used on various materials, including cast irons, steels, aluminum alloys and titanium alloys [11]. In addition to these materials, Kumara et al. [12] applied DR on IS 319-2007 brass and reported up to 75% reduction in roughness. In recent literature, DR applications on aluminum alloys have increased. Abdulstaar et al. [13] applied DR on 6082 aluminum alloy. They reported a hardness increase of up to 21% and a 140% fatigue strength improvement after DR. Beghini et al. [14] showed that surface roughness decreased significantly after DR. The post-DR roughness was found to be dependent on pre-DR roughness values for 7075 aluminum alloy. They also reported compressive residual stresses reaching 1 mm depth after DR. In the work of Bataineh et al. [15], 6061-T6 aluminum alloy's hardness and roughness responses to different parameters were investigated after DR employing ANOVA. Similarly, Barahate et al. [16] have performed experiments to investigate the effects of rolling speed, feed rate, and rolling force on hardness and

roughness values. Celik et al. [17] investigated the influence of DR force on fatigue strength for the 7075-T6 aluminum alloy. They showed that 80 N and 121 N deep rolling forces resulted in significant fatigue strength increase, whereas 242 N rolling force resulted in lower fatigue life than 80 N and 121 N force cases. The deep rolling tool in their study was Yamato SKUV 20-2, 5R80, and the rotating-bending fatigue specimens had a 4 mm gage diameter.

Deep rolling-induced residual stresses were shown to be different in different directions in the study of Coules et al. [18]. Similarly, Beghini et al. [14] showed that induced residual stresses on a 7075 aluminum flat surface depend on the DR direction when a roller-type DR tool is used. Therefore, investigating the effects of DR direction on specimens' fatigue properties is of technological importance. Conventionally, DR direction is chosen as the turning direction, and feed is given in the direction parallel to the longitudinal axis of axisymmetric parts [8]. However, the authors believe that a configuration in which the rolling is in the longitudinal axis direction and the feed is in the turning direction can improve the fatigue properties even further. This configuration exploits the fact that residual stresses are dependent on the DR application direction. El-Tayeb et al. [19] used this configuration to investigate the tribological properties of 6061 aluminum alloy. However, no attempt was presented in their work to investigate residual stresses and fatigue properties. In the current study, the fatigue properties of EN-AW 6082-T6 aluminum alloy, which is extensively used in the automotive industry, were investigated using different DR directions.

2.0 MATERIAL AND EXPERIMENTAL METHODS

2.1 Materials

The 6082 aluminum alloy rods with 15 mm diameter and 120 mm length were used to manufacture specimens in this study. The chemical composition of the alloy is shown in Table 1. The Mg and Si elements in the composition enable precipitation hardening after a procedure known as artificial aging [20]. Therefore, solution heat treatment was applied at 550°C for 90 minutes, followed by an immediate quench. Specimens were transferred to another furnace held at 180°C within 1 minute after quenching and artificially aged for 480 minutes, obtaining T6 temper.

Table 1. Chemical Composition of 6082 Alloy [wt%]

Mg	Si	Mn	Fe	Zn	Cu	Ti	Al
1.00	0.93	0.53	0.30	0.083	0.015	0.012	Remainder

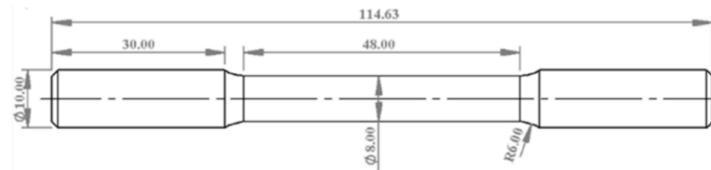


Figure 1. Tensile test specimen geometry (dimensions in mm)

Tensile tests were conducted to determine the mechanical properties of the used alloy according to ISO 6892-1 standard. Tensile test specimen geometry is shown in Figure 1. Tests were done on three specimens, and relevant data were averaged. A strain rate of 1×10^{-3} was used. Tensile test results of the alloy can be examined in Table 2.

Table 2. Tensile test results of 6082 aluminum alloy

Yield strength (MPa)	Tensile strength (MPa)	Elongation (%)
280.8 ± 5.9	312.0 ± 9.8	22.3 ± 1.4

2.2 Experimental method

Specimens with the geometry shown in Figure 2 were manufactured for roughness, hardness, and fatigue strength measurements. A CNC turning machine (Model: SPINNER TC600) was utilized to apply deep rolling on these specimens. Yamato SKUV 20-2,5R-80 DR tool was used in this study, similar to the work of Celik et al. [17]. Two different DR directions were employed; longitudinal rolling (LR) and tangential rolling (TR), as shown in Figure 3. For both applications, rolling speed, rolling force, and feed rate were selected as 10 mm/s, 250 N, and 0.1 mm/pass, respectively. Feed was applied continuously by employing constant turret movement during rolling for TR. Whereas for LR, it was given discretely after each rolling pass by turning the specimen by an angle of 1.43° , corresponding to 0.1 mm/pass. The complete surface of the gage section was deep rolled for each specimen.

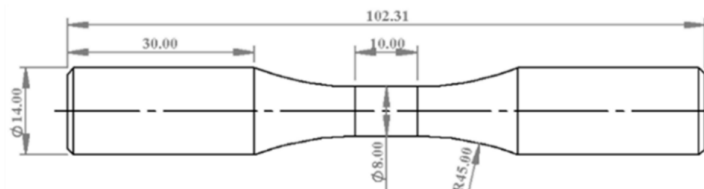


Figure 2. Fatigue specimen geometry (dimensions in mm)

Roughness measurements of specimens were conducted in compliance with the ISO 4287-1997 standard. A Mitutoyo SJ-210 roughness measurement apparatus was employed in the experiments. One specimen from each set was used to measure roughness values. Ten readings were taken on each specimen in the direction of the longitudinal axis of the specimens, and the data were averaged. Hardness measurements were conducted following the suggestions in the ISO 6507-1 standard using a Future-Tech FM-700e Vickers hardness tester. A section from one untested fatigue specimen was cut using abrasive cutting for both TR and LR. Sectioned specimens were cold-mounted in epoxy resin and ground using 240-400-800-1200-2500 grit sandpapers. Afterwards, polishing was performed on these specimens using 6 μm and 1 μm diamond solutions successively. During hardness tests, a 10 g load and a dwell time of 15 seconds were used to appropriately capture the spatial resolution of hardness distribution within the cross-sections of specimens. The fatigue test was performed according to ASTM E466-07 standard. Fully-reversed, stress-controlled cycles were used in a servo-hydraulic axial fatigue testing machine (BESMAK) to obtain fatigue responses up to 2 million cycles. The S-N curves were derived using the least-squares regression method. Fractured surfaces of the selected fatigue specimens were examined utilizing scanning electron microscopy (SEM) using an FEI Quanta 200 model microscope. An accelerating voltage of 15 kV was used in these investigations.

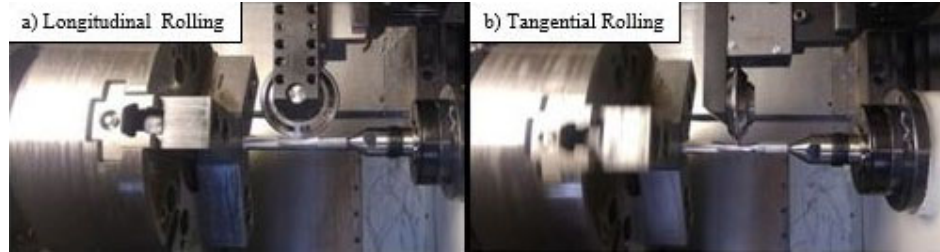
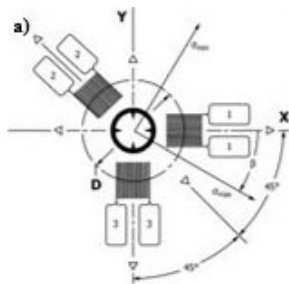


Figure 3. Deep rolling process: (a) longitudinal rolling; (b) tangential rolling

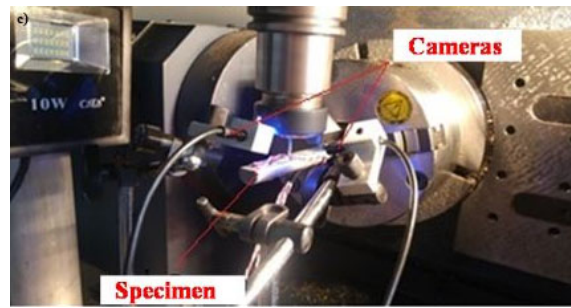
The hole-drilling method was employed to study the residual stress distribution in depth direction after deep rolling. Details of this method are explained in the ASTM E837-08 standard. In this method, a specifically designed strain-gage rosette is used on the surface, and a hole is drilled incrementally. After each increment, the drilling process is stopped, and strain-gage readings are recorded. At the end of the entire process, recorded strain readings are used to calculate corresponding residual stresses employing calibration matrices that were determined using finite element simulations, as explained in the work of Schajer [21]. High-speed drilling (up to 300,000 rpm) procedures using air turbines are generally recommended by the ASTM E837-08 standard for the hole drilling method to minimize residual stresses arising from the drilling process. However, the use of conventional CNC milling machines for the hole-drilling technique was employed by Nobre et al. [22] for carbon-epoxy laminate composite and by Alinaghian et al. [23] for Al/Cu bimetal specimens with satisfactory results. Therefore, a conventional CNC milling machine (Model: SPINNER VC560) was used to drill a hole in the specimens for the strain gage measurements in the current study. A single deep-rolled flat specimen was used in the measurements. ASTM E837-Type-A 031-RE strain gages were utilized. The hole diameter for this strain gage type is 1 mm. A turning speed of 25000 rpm and a feed rate of 1 $\mu\text{m}/\text{s}$ were used for drilling to minimize the effects of the drilling process on residual stresses. Figures 4(a) and 4(b) display the schematic drawing of the strain gage and its application on a flat surface, respectively. The experimental setup can be examined in Figure 4(c). In this setup, two perpendicular cameras were employed to accurately position the specimen in such a way that misalignments between the strain-gage center and the drilled hole could be minimized. Measurements were carried out up to 350 μm depth using six increments.



(a) schematic of a strain-gage rosette,



(b) strain-gage application on surface, and



(c) experimental setup for residual stress measurements

Figure 4. Hole drilling method application using conventional CNC milling machine

3.0 RESULTS AND DISCUSSION

Figure 5 displays the mean roughness values (Ra) and mean roughness depths (Rz) for as-turned (AT), TR, and LR specimens. Error bars represent standard deviations. It can be seen that Ra and Rz values decreased drastically after deep rolling. A two-tailed t-test was performed on the measurement data sets of TR and LR using a two-sample unequal variance approach. The respective p-values for Ra and Rz were 0.0575 and 0.246, both of which were higher than $p=0.05$. Therefore, a meaningful difference in the roughness values was not present between the TR and LR cases. Ra values were reduced from approximately $0.7 \mu\text{m}$ to $0.1 \mu\text{m}$, whereas Rz values were reduced from $2.7 \mu\text{m}$ to $0.5 \mu\text{m}$. Moreover, scatter within roughness readings was also reduced considerably, which indicates sufficient reproducibility. These results suggest that both rolling directions can be used to improve surface quality.

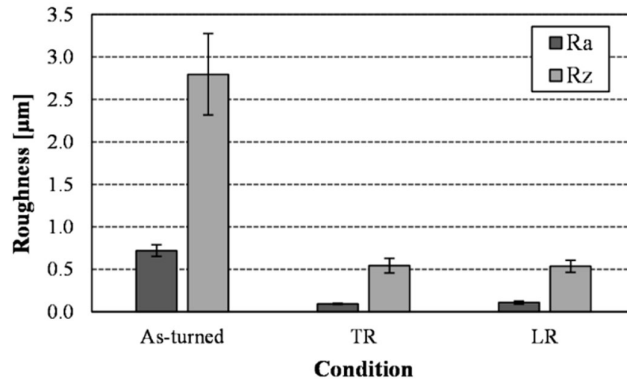


Figure 5. Roughness measurement results

Work-hardening in the surface region is a significant aspect of deep-rolled components. Figure 6 displays hardness readings obtained after both TR and LR. The specimens' bulk material hardness was 123 HV. Both TR and LR resulted in a considerable hardness increase in the surface region. Additionally, there was no significant difference between the hardness values for the investigated rolling direction applications. TR and LR yielded an approximately 10% hardness increase near the surface, and work-hardened regions up to approximately 1 mm depth were observed. Since work-hardening hinders slip in crystals, fatigue crack initiation can be expected to be delayed after both deep rolling applications.

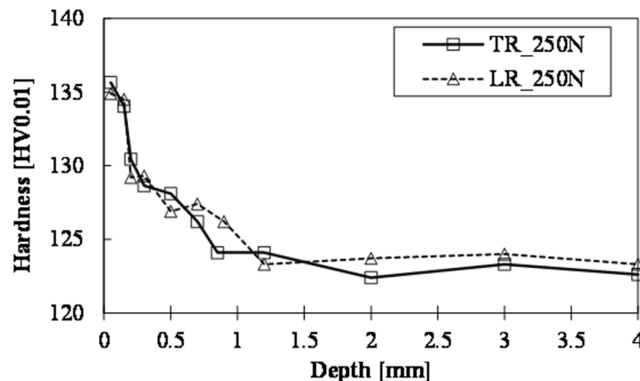


Figure 6. Hardness distribution after deep rolling

Figure 7 shows deep rolling-induced residual stresses for a flat surface. Obtained residual stresses were below the yield strength of the alloy, indicating that the measurements were suitable. Significant differences in residual stress profiles were observed in two perpendicular directions. The compressive residual stress values near the surface were higher in the rolling direction than in the feed direction. Most of the fatigue life is spent during the crack initiation phase for HCF, and fatigue cracks usually form at component surface. Therefore, HCF strength can be expected to reach higher levels compared to the feed direction when external loading is in the same direction as the rolling direction. Tensile residual stresses are expected after some depth to balance the compressive ones. However, the measurement range was not sufficient to capture those stresses.

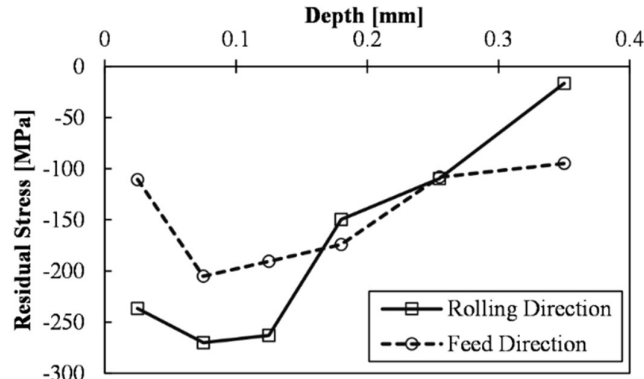


Figure 7. Residual stress distribution on flat surface after deep rolling

Fatigue strength improvement is the main reason to apply deep rolling to components. Figure 8 shows the results of the fatigue experiments in the current study. It is seen that the HCF lives of specimens increased after deep rolling. This increase was more pronounced in the LR specimens than in the TR ones. Fatigue strength at 10^6 cycles was determined to be 136 MPa for the as-turned (AT) condition. Fatigue strengths of 145 MPa after TR and 167 MPa after LR were obtained, corresponding to 7% and 23% fatigue strength improvements, respectively. Since roughness and hardness results were not significantly affected by changing the deep rolling direction, differences between the fatigue results of TR and LR can be explained by the residual stress changes. Higher compressive residual stresses in the rolling direction may improve fatigue strength when external loading is in the same direction, which was the case for the LR fatigue specimens. For the TR application, the fatigue load was applied in the lower compressive residual stress direction, which resulted in less fatigue strength than the LR application. Differences in fatigue strengths between TR and LR show that the direction dependency of residual stresses plays a crucial role in the deep rolling process and the resulting fatigue behavior. Furthermore, scatters of fatigue data were significantly lower for both TR and LR compared to AT. The correlation coefficient (R^2) for the S-N curve of AT was 0.58, whereas this value was 0.73 for TR and 0.87 for LR. The scatter of fatigue data, especially at the HCF regime, is a major design factor and is therefore of high technological importance [24].

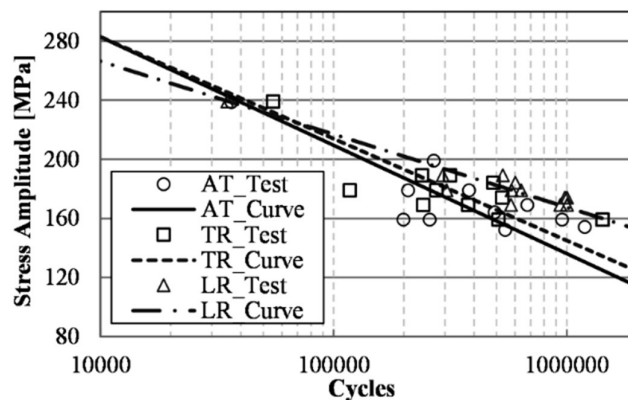


Figure 8. Fatigue test results and corresponding S-N diagrams

Figures 9 to 11 show the SEM images of the AT, TR, and LR specimens, respectively. For the AT specimen, crack initiation took place at the surface, as seen in Figure 9(b). Surface crack initiation was expected since fatigue cracks usually start at the free surface, where irregularities and defects are present. Figure 9(c) shows the fatigue striations close to the crack initiation site. These striations show the crack fronts after each cycle during crack propagation [24]. After a certain crack length, the specimen could not resist the load and fractured from the remaining material, as seen in Figure 9(d).

Figures 10(b) and 11(b) show sub-surface crack initiation regions for TR and LR specimens, respectively. Near crack initiation sites, a wave-like texture was present in both cases. This type of topography was not present in the AT specimen. This texture is believed to be the result of shear deformation pile-ups and deepened persistent slip bands during crack initiation. The presence of this texture and the fact that crack initiation occurred in the sub-surface region indicate that crack initiation was hindered for a significant amount of time, which resulted in higher fatigue lives. Therefore, it can be said that surface region properties after deep rolling allow for delaying the crack initiation phase, which results in improved fatigue life.

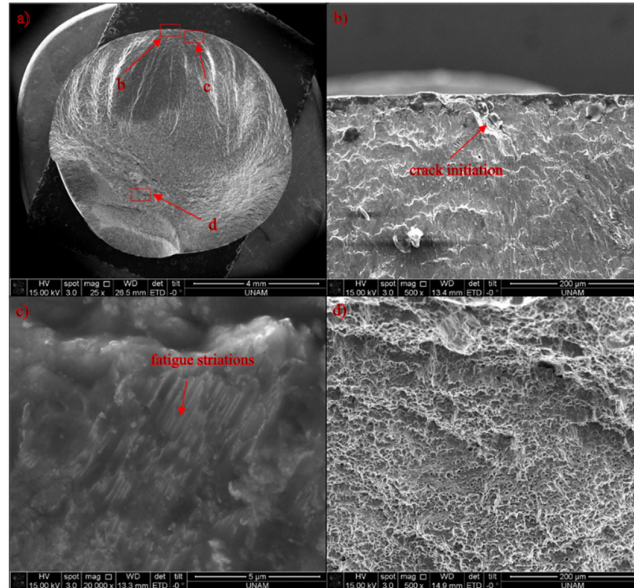


Figure 9. SEM images of AT specimen fractured under $\sigma_a=160$ MPa; (a) general view, (b) crack initiation zone, (c) fatigue striations close to crack initiation zone and (d) sudden fracture zone

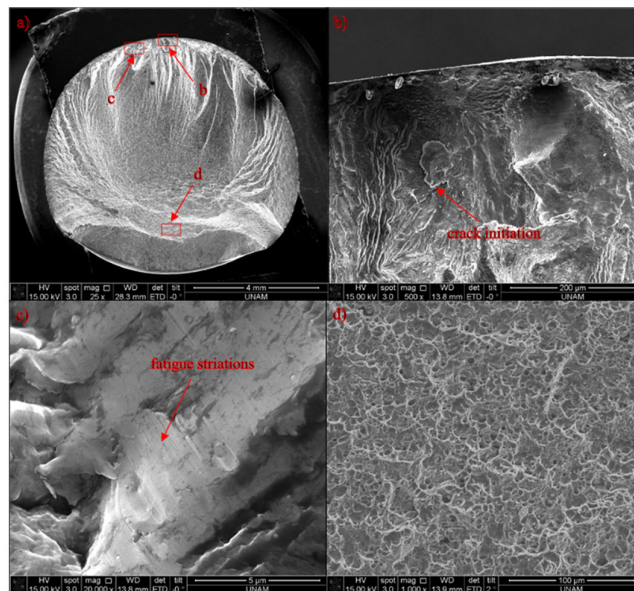


Figure 10. SEM images of TR specimen fractured under $\sigma_a=160$ MPa; (a) general view, (b) crack initiation zone, (c) fatigue striations close to crack initiation zone and (d) sudden fracture zone

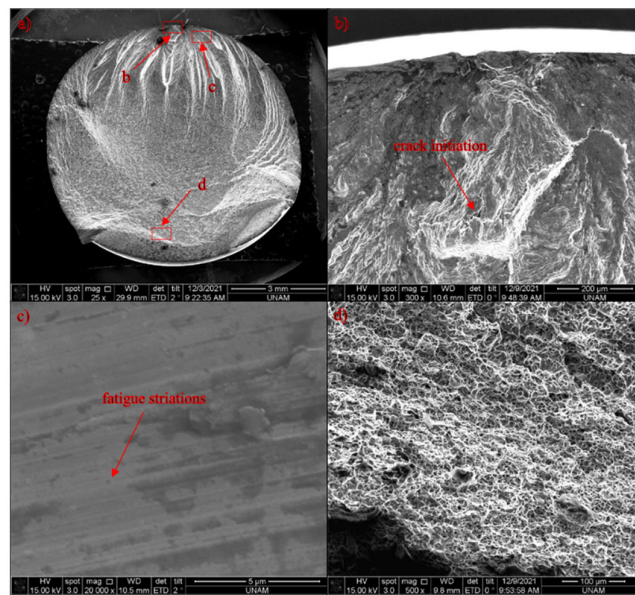


Figure 11. SEM images of LR specimen fractured under $\sigma_a=160$ MPa; (a) general view, (b) crack initiation zone, (c) fatigue striations close to crack initiation zone and (d) sudden fracture zone

4.0 CONCLUSIONS

Deep rolling on EN-AW 6082 aluminum alloy was investigated by employing different rolling directions. For the investigated processing conditions, the surface roughness decreased after deep rolling. There was no significant difference between the roughness values after deep rolling in the tangential and longitudinal directions. Similarly, hardness increases in the surface region after both TR and LR were similar, and an approximately 10% increase in hardness was present at the surface for both cases. Contrary to roughness and hardness, residual stresses generated after deep rolling depended significantly on the deep rolling direction. Measurements on a deep-rolled flat surface showed that compressive residual stresses in the rolling direction were considerably larger near the surface compared to the feed direction.

Fatigue strength improvements were possible after TR and LR. However, improvement in fatigue strength was more pronounced for LR than for TR. Fatigue strength improvements of 7% and 23% were possible for TR and LR, respectively. This difference can be justified when the dissimilarities in the residual stresses between TR and LR are considered. Compressive residual stresses of higher magnitude develop in the rolling direction compared to the feed direction. Since the rolling direction is the same as the fatigue loading direction for LR, higher fatigue strength values can be expected for LR compared to TR. SEM images showed that fatigue cracks initiated at the surface for the AT specimen, whereas sub-surface crack initiation was observed for both the TR and LR specimens. Therefore, both deep rolling applications resulted in a delayed crack initiation phase and increased HCF life.

5.0 ACKNOWLEDGEMENT

The authors would like to thank the Turkish Scientific and Technological Research Council (TÜBİTAK) for funding this work under Project: 217M962.

6.0 REFERENCES

- [1] M.N. Sakib, and A.A. Iqba, "Epoxy based nanocomposite material for automotive application-a short review," *International Journal of Automotive and Mechanical Engineering*, vol. 18, no. 3, pp. 9127–9140, 2021.
- [2] M. Kleiner, M. Geiger, and A. Klaus, "Manufacturing of lightweight components by metal forming," *CIRP Annals*, vol. 52, no. 2, pp. 521-542, 2003.
- [3] L. Kukielka, "Designating the field areas for the contact of a rotary burnishing element with the rough surface of a part, providing a high-quality product," *Journal of Mechanical Working Technology*, vol. 19, no. 3, pp. 319-356, 1989.
- [4] A. Purnowidodo, ss. Arief, and FH. Iman, "Effect surface roughness on fatigue crack propagation behaviour of fibre Metal Laminates (FMLs)," *International Journals of Automotive and Mechanical Engineering*, vol. 16, no. 2, pp. 6588-6604, 2019.
- [5] K. Kirkhope, R. Bell, L. Caron, R. Basu, and K-T Ma, "Weld detail fatigue life improvement techniques," *Part 1. Marine structures*, vol. 12, no. 6, pp. 447-474, 1999.
- [6] L. Wagner, "Mechanical surface treatments on titanium, aluminum and magnesium alloys," *Materials Science and Engineering: A.*, vol. 263, no. 2, pp. 210-216, 1999.
- [7] T. Ludian, and L. Wagner, "Mechanical surface treatments for improving fatigue behavior in titanium alloys," *Advances in Materials Science*, vol. 8, no. 2, pp. 44, 2008.
- [8] V. Schulze, *Modern mechanical surface treatment: States, stability, effects*, John Wiley & Sons; 2006.

- [9] R. Nalla, I. Altenberger, U. Noster, G. Liu, B. Scholtes, and R. Ritchie, "On the influence of mechanical surface treatments—deep rolling and laser shock peening—on the fatigue behavior of Ti–6Al–4V at ambient and elevated temperatures," *Materials Science and Engineering: A.*, vol. 355, no. 1-2, pp. 216-230, 2003.
- [10] S. Bagherifard, I. Fernandez-Pariente, R. Ghelichi, and M. Guagliano, "Effect of severe shot peening on microstructure and fatigue strength of cast iron," *International Journal of Fatigue*, vol. 65, pp. 64-70, 2014.
- [11] P. Delgado, I. Cuesta, J. Alegre, and A. Díaz, "State of the art of Deep Rolling," *Precision Engineering*, vol. 46, pp. 1-10, 2016.
- [12] P. Kumara, and G. Purohit, "Improving surface roughness of burnished components using abrasive particles," *International Journal of Automotive and Mechanical Engineering*, vol. 15, no. 3, pp. 5592-5606, 2018.
- [13] M. Abdulstaar, M. Mhaede, and L. Wagner, "Pre-corrosion and surface treatments effects on the fatigue life of AA6082 T6," *Advanced Engineering Materials*, vol. 15, no. 10, pp. 1002-1006, 2013.
- [14] M. Beghini, L. Bertini, B.D. Monelli, C. Santus, and M. Bandini, "Experimental parameter sensitivity analysis of residual stresses induced by deep rolling on 7075-T6 aluminium alloy," *Surface and Coatings Technology*, vol. 254, pp. 175-186, 2014.
- [15] O. Bataineh, "Effect of roller burnishing on the surface roughness and hardness of 6061-T6 aluminum alloy using ANOVA," *International Journal of Mechanical Engineering and Robotics Research*, vol. 8, no. 4, 2019.
- [16] V. Barahate, A.R. Govande, G. Tiwari, B.R. Sunil, and R. Dumpala, "Parameter optimization during single roller burnishing of AA6061-T6 alloy by design of experiments," *Materials Today: Proceedings*, vol. 50, pp. 1967-1970, 2022.
- [17] M. Celik, U. Caydas, and M. Akyuz, "The influence of roller burnishing process parameters on surface quality and fatigue life of AA 7075-T6 alloy," *Materialwissenschaft und Werkstofftechnik*, vol. 53, no. 5, pp. 608-616, 2022.
- [18] H. Coules, G. Horne, S. Kabra, P. Colegrove, and D. Smith, "Three-dimensional mapping of the residual stress field in a locally rolled aluminium alloy specimen," *Journal of Manufacturing Processes*, vol. 26, pp. 240-251, 2017.
- [19] N. El-Tayeb, K. Low, and P. Brevern, "Influence of roller burnishing contact width and burnishing orientation on surface quality and tribological behaviour of Aluminium 6061," *Journal of Materials Processing Technology*, vol. 186, no. 1-3, pp. 272-278, 2007.
- [20] A. Cuniberti, A. Tolley, M.C. Riglos, R. Giovachini, "Influence of natural aging on the precipitation hardening of an AlMgSi alloy," *Materials Science and Engineering: A.*, vol. 527, no. 20, pp. 5307-5311, 2010.
- [21] G. Schajer, "Measurement of non-uniform residual stresses using the hole-drilling method. Part II—practical application of the integral method," *Journal of Engineering Materials and Technology*, vol. 110, no. 4, pp. 338-343, 1988.
- [22] J.P. Nobre, J. Stiffel, W.V. Paepegem, A. Nau, A.C. Batista, et al., "Quantifying the drilling effect during the application of incremental hole-drilling technique in laminate composites," *Materials Science Forum*, vol. 681, pp.510-515, 2011.
- [23] M. Alinaghian, I. Alinaghian, and M. Honarpisheh, "Residual stress measurement of single point incremental formed Al/Cu bimetal using incremental hole-drilling method," *International Journal of Lightweight Materials and Manufacture*, vol. 2, no. 2, pp. 131-139, 2019.
- [24] G.E. Dieter, and D. Bacon, *Mechanical metallurgy*. New York: McGraw-Hill New York, 1976.